CHEMISTRY OF MATERIALS
Article

Chem. Mater. **2010,** *22,* 3067–3071 3067
DOI:10.1021/cm9036428

Inkjet Printing of Conductive Silver Patterns by Using the First Aqueous Particle-Free MOD Ink without Additional Stabilizing Ligands†

Stephan F. Jahn, Thomas Blaudeck, and Reinhard R. Baumann*

Institute for Print and Media Technology, Chemnitz University of Technology, Reichenhainer Strasse 70, 09126 Chemnitz, Germany

Alexander Jakob, Petra Ecorchard, Tobias Rüffer, and Heinrich Lang*

Faculty of Natural Sciences, Department of Inorganic Chemistry, Chemnitz University of Technology, Strasse der Nationen 62, 09111 Chemnitz, Germany

Peer Schmidt

Inorganic Chemistry, Dresden University of Technology, Helmholtzstrasse 10, 01069 Dresden, Germany

Received December 2, 2009. Revised Manuscript Received April 1, 2010

The chemical and physical properties of $[AgO_2C(CH_2OCH_2)_3H]$ (**3**) and its use as an aqueous, ligand-free MOD ink (MOD = metal−organic decomposition) for piezo inkjet printing is discussed. The printed, thermal, or photochemical sintered silver features are electrically conductive on glass (2.7×10^7 S m^{-1}) and PET (PET = polyethylene terephthalate) substrates (1.1×10^7 S m^{-1}) corresponding to 43% and 18% of the bulk silver conductivity. Conducted tape tests show the suitability of the ink for particularly polymer substrates. TG-MS studies demonstrate a two-step decomposition for the conversion of **3** to elemental silver. The structure of **3** in the solid state was determined by single X-ray structure determination.

1. Introduction

Silver(I) complexes of type $[L_nAgX]$ (L = two-electron donor; $n = 1, 2, 3$; X = halide, pseudohalide, single-bonded organic group) serve as precursors for metallization processes using deposition techniques such as CVD (chemical vapor deposition), ALD (atomic layer deposition), and spin- and dip-coating.[1] Suitable precursors are particularly phosphane and phosphite silver(I) carboxylates because they produce thin, highly pure, and dense silver layers of high conductivity on diverse substrate materials, which is of importance for micro- and nanoelectronic industries. Bokhonov and Olson studied the decomposition behavior of these metal−organic coordination complexes forming metallic silver islands during the thermal transition process.[2−4] Temperature-dependent and in situ mass spectrometry (volatile materials) and thermogravimetric mass spectrometry (TG-MS) measurements (nonvolatile compounds) were reported by our group.[5]

Nevertheless, for most flexible substrates to be metallized, the thermal conversion of silver(I) complexes is a challenge because the respective approaches have to cope with the limited thermal stability of the appropriate polymeric substrate material. For flexible substrates such as polyethylene terephthalate (PET), the applied temperature during fabrication plays a decisive role because the precursor material must decompose before the substrate starts to soften. To manufacture conducting electrodes for connections between organic devices and large-area electronics, imagewise metallization of flexible substrates is required. In contrast to patterning technologies including

† Dedicated to Prof. Dr. Uwe Rosenthal on the occasion of his 60th birthday.

*To whom correspondence should be addressed. For R.R.B.: e-mail, reinhard.baumann@mb.tu-chemnitz.de; phone, 0371/531-35843; fax, 0371/531-8-35843. For H.L.: e-mail, heinrich.lang@chemie.tu-chemnitz.de; phone, 0371/531-21210; fax, 0371/531-21219.

(1) (a) Szczesny, R.; Szymanska, I.; Piszczek, P.; Dobrzanska, L.; Szlyk, E. *Mater. Sci. Pol.* **2005**, *23*(3), 671–676. (b) Niskanen, A.; Hatanpaa, T.; Arstila, K.; Leskela, M.; Ritala, M. *Chem. Vap. Deposition* **2007**, *13*(8), 408–413. (c) Jakob, A.; Schmidt, H.; Walfort, B.; Rheinwald, G.; Frühauf, S.; Schulz, S.; Gessner, T.; Lang, H. *Z. Anorg. Allg. Chem.* **2005**, *631*, 1079–1086. (d) Jakob, A.; Schmidt, H.; Djiele, P.; Shen, Y.; Lang, H. *Microchim. Acta* **2006**, *156*(1−2), 77–81. (e) Grodzicki, A.; Lakomska, I.; Piszczek, P.; Szymanska, I.; Szlyk, E. *Coord. Chem. Rev.* **2005**, *249*(21−22), 2232–2258. (f) Schmidt, H.; Shen, Y.; Leschke, M.; Haase, T.; Kohse-Hoinghaus, K.; Lang, H. *J. Organomet. Chem.* **2003**, *669*(1−2), 25–31. (g) Edwards, D. A.; Mahon, M. F.; Molloy, K. C.; Ogrodnik, V. *J. Mater. Chem.* **2003**, *13*(3), 563–570. (h) Edwards, D. A.; Harker, R. M.; Mahon, M. F.; Molloy, K. C. *Inorg. Chim. Acta* **2002**, *328*, 134–146. (i) Li, Y. U.S. Pat. Appl. Publ. US 2009140336 A1 20090604, **2009**

(2) Bokhonov, B. B.; Sidelnikov, A. A.; Sharafutdinov, M. R.; Tolochko, B. P.; Burleva, L. P.; Whitcomb, D. R. *J. Imaging Sci. Technol.* **2003**, *47*(2), 89–99.

(3) Olson, L. P.; Whitcomb, D. R.; Rajeswaran, M.; Blanton, T. N.; Stwertka, B. J. *Chem. Mater.* **2006**, *18*, 1667–1674.

(4) Bokhonov, B. B.; Sharafutdinov, M. R.; Tolochko, B. P.; Burleva, L. P.; Whitcomb, D. R. *J. Imaging Sci. Technol.* **2007**, *51*(4), 386–390.

(5) (a) Haase, T.; Kohse-Hoeinghaus, K.; Atakan, B.; Schmidt, H.; Lang, H. *Chem. Vap. Deposition* **2003**, *9*(3), 144–148. (b) Haase, T.; Kohse-Hoeinghaus, K.; Bahlawane, N.; Djiele, P.; Jakob, A.; Lang, H. *Chem. Vap. Deposition* **2005**, *11*(4), 195–205.

Published on Web 04/21/2010

photolithography and shadow-mask evaporation, inkjet printing of functional inks is an alternative technique. This additive technology requires rather low-level investments and additionally can be operated under ambient conditions. Silver inkjet inks are available as a dispersion of nanoparticles.[6−8] The disadvantage of the dispersion inks are the particles themselves (i) determining the nozzle diameters of the inkjet heads and therefore the minimal feature size of the patterns and (ii) showing a tendency to clog in the microfluidic system of the inkjet head when their diameter exceeds 1% of the nozzle diameter.[12] Another strategy is the use of metal−organic complexes in solution as decomposition inks (MOD inks),[9−14] for example, [$AgNO_3$] dissolved in water was applied as ink.[13,14] However, the disadvantage of this system is its high light sensitivity. Additionally, [$AgNO_3$] decomposes at high temperature (440 °C). MOD inks require as post-treatment thermal sintering, whereby the appropriate metal−organic species are converted to conductive silver layers by the in situ formation of Ag nanoparticles. Further low temperature processes for Ag inks are microwave[15] and laser-assisted sintering,[16,17] chemical conversion,[17,18] electrical sintering,[19] UV radiation,[20] and plasma treatment.[21]

We describe here the utilization of the metal−organic silver salt [$AgO_2C(CH_2OCH_2)_3H$] for the formulation of an aqueous MOD ink suitable for inkjet patterning of conductive silver features on glass and flexible substrate materials such as PET by applying thermal or photothermal treatments. The thermal decomposition mechanism of [$AgO_2C(CH_2OCH_2)_3H$] was investigated by TG-MS studies (TG = thermogravimetry).

2. Results and Discussion

Silver(I) 2-[2-(2-methoxyethoxy)ethoxy]acetate (**3**), which is stable to air, was available by the reaction of the silver salt [$AgNO_3$] (**1**) with $HO_2C(CH_2OCH_2)_3H$ (**2**) in the presence of NEt_3 in a mixture of ethanol−acetonitrile in the ratio of 20:1 (v/v) at ambient temperature (reaction 1).[22]

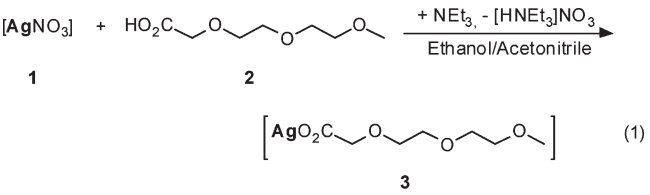

Complex **3** was characterized by elemental analysis, IR, and NMR spectroscopy and mass spectrometry. The thermal decomposition behavior was studied by TG/DTG (thermogravimetry/differential thermogravimetry) and DSC (differential scanning calorimetry). Additionally, the structure of **3** in the solid state was established by single X-ray structure determination (Supporting Information).

The thermal decomposition of solid **3** was studied by TG-MS coupling experiments. Also, differential scanning calorimetric measurements were carried out.[22] The corresponding TG/DTG and DSC response curves (argon, temperature range of 25−500 °C, heating rate of 10 K min^{-1}) are depicted in Figure 1.

The thermal decomposition of **3** is detectable at > 200 °C and occurs in two adjacent steps (Figure 1). The first step shows a mass loss $\Delta m/m_0$ of −37(1)%, while the second step proceeds with −25(1)%. The overall mass diminution with −62(1)% corresponds to the formation of elemental silver ($\Delta m/m_0$ = 62% experimental and theoretical). Similar results were obtained for silver(I) carboxylates of general type [L_nAgO_2CR] (L = phosphane, phosphite; n = 1, 2, 3; R = single-bonded organic group).[5] The DSC curve depicted in Figure 1 shows two endothermic processes at 78 and 107 °C, respectively, relating most probably to a phase transformation and melting of **3**. The thermal decomposition of **3** starts with an exothermic effect at ∼200 °C which may result from the oxidation of carbon monoxide or hydrogen carbons CH_x toward carbon dioxide.

TG-MS investigations were carried out to get a deeper insight into the decomposition mechanism of **3** (Figure 2, Table 1). TG-MS coupling studies show that carbon dioxide is eliminated first, indicating cleavage of the Ag−O bond. Recombination of the thus formed organic fragment results in the formation of a silver(I) alkyl species. Most probably, the in situ formed organics are

(6) Fuller, S. B.; Wilhelm, E. J.; Jacobson, J. M. *J. Microelectromech. Syst*. **2002**, *11*(1), 54–60.
(7) Lee, K. J.; Jun, B. H.; Kim, T. H.; Joung, J. *Nanotechnology* **2006**, *17*, 2424–2428.
(8) (a) Kamyshny, A.; Ben-Moshe, M.; Aviezer, S.; Magdassi, S. *Macromol. Rapid Commun*. **2005**, *26*, 281–288. (b) Aminuzzaman, M.; Watanabe, A.; Miyashita, T. *Thin Solid Films* **2009**, *517*, 5935–5939.
(9) Teng, K. F.; Vest, R. W. *IEEE Electron Device Lett*. **1988**, *9*(11), 591–593.
(10) Dearden, A. L.; Smith, P. J.; Shin, D.-Y.; Reis, N.; Derby, B.; O'Brien, P. *Macromol. Rapid Commun*. **2005**, *26*, 315–318.
(11) Smith, P. J.; Shin, D.-Y.; Stringer, J. E.; Derby, B.; Reis, N. *J. Mater. Sci*. **2006**, *41*, 4153–4158.
(12) Romano, F. J. *Inkjet! History, Technology, Markets, and Applications*; Digital Printing Council PIA/GATFPress: Pittsburgh, PA, 2008.
(13) Mei, J.; Lovell, M. R.; Mickle, M. H. *IEEE Trans. Electron. Packag. Manuf*. **2005**, *28*(3), 265–273.
(14) (a) Xue, F.; Liu, Z.; Su, Y.; Varahramyan, K. *Microelectron. Eng*. **2006**, *83*, 298–302. (b) Wu, J.-T.; Hsu, S. L.-C.; Tsai, M.-H.; Hwang, W.-S. *Thin Solid Films* **2009**, *517*, 5913–5917.
(15) Perelaer, J.; de Gans, B.-J.; Schubert, U. S. *Adv. Mater*. **2006**, *18*, 2101–2104.
(16) Yung, K. C.; Wu, S. P.; Liem, H. *J. Mater. Sci*. **2009**, *44*(1), 154–159.
(17) Smith, P. J.; Mager, D.; Löffelmann, U.; Korvink, J. G. *Proceedings of NIP24 and Digital Fabrication 2008*; Pittsburgh, PA, 2008; IS&T and ISJ: Springfield, VA, and Japan, 2008; pp 689−692.
(18) Zapka, W.; Voit, W.; Loderer, C.; Lang, P. *Proceedings of NIP24 and Digital Fabrication 2008*, Pittsburgh, PA, 2008; IS&T and ISJ: Springfield, VA, and Japan, 2008; pp 906−911.
(19) Allen, M. L.; Aronniemi, M.; Mattila, T.; Alastalo, A.; Ojanperä, K.; Suhonen, M.; Seppä, H. *Nanotechnology* **2008**, *19*, 175201.
(20) Radivojevic, Z.; Andersson, K.; Hashizume, K.; Heino, M.; Mantysalo, M.; Mansikkamaki, P.; Matsuba, Y.; Terada, N. *Proceedings of THERMINIC*, Côte d'Azur, France, 2006, EDA Publishing Association: Grenoble, France, 2006; pp 163−168.
(21) Reinhold, I.; Hendricks, C. E.; Eckhardt, R.; Kranenburg, J. M.; Perelaer, J.; Baumann, R. R.; Schubert, U. S. *J. Mater. Chem*. **2009**, *19*(Suppl.), 3384–3388.
(22) Steffan, M.; Jakob, A.; Claus, P.; Lang, H. *Catal. Commun*. **2009**, *10*, 437–441.

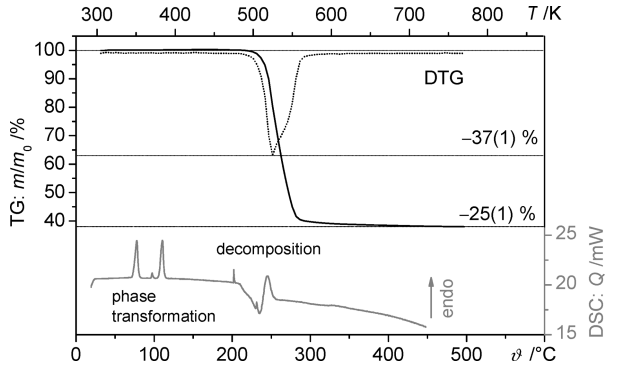

Figure 1. TG/DTG (top) and DSC (bottom) traces for the thermal heating of **3** in argon (flow rate of 100 mL min^{-1}) with a temperature increase of 10 K min^{-1}.

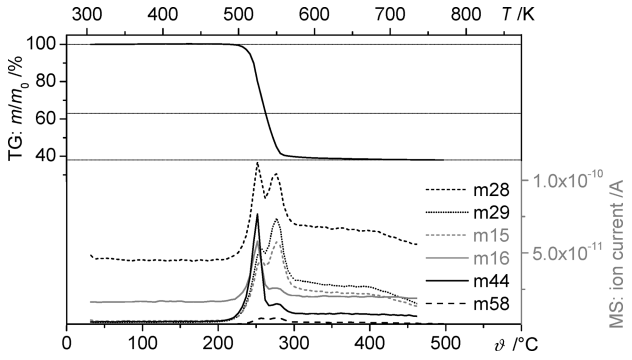

Figure 2. Mass spectrometric scans of the thermal induced decomposition of **3**: $m/z = 15$ (CH_3^+); $m/z = 16$ (CH_4^+); $m/z = 28$ (CO^+); $m/z = 29$ (CHO^+); $m/z = 44$ (CO_2^+); $m/z = 58$ ($C_2H_2O_2^+$).

responsible for the narrow distribution of the Ag nanoparticles.[23] Also, the evolution of CO and gaseous $C_xH_yO_z$ ($x \geq 3$) species can be detected in both decompositions by mass spectrometry. After decarboxylation of **3**, the in situ formed organometallic silver(I) alkyl derivative decomposes via Ag−C, C−C, and C−O homolytical bond cleavage processes. However, it cannot be ruled out that an oxygen attack on the silver(I) ion(s) from the oligoether fragments takes place and further decompositions from such species occur.

A 23% aqueous MOD ink based on colorless silver(I) carboxylate **3**[22] was formulated by dissolving **3** in water. This leads to a silver content of 9.1% in the ink possessing a viscosity of 1.9 mPas and a surface tension of 60 mN m^{-1} at 20 °C.

Inkjet printing experiments were conducted with a Dimatix materials printer DMP2831 (21.5 μm nozzle diameter) on glass object slides. For sintering the printed structures, a heating plate was set to 250 °C following the TG and DSC characteristics. First, the appearance of single droplets was studied. Depending on the settings on the printer, the print-head ejects droplets between 5 and 10 pL. A 3D profile of a single nonsintered droplet (Figure 3a) shows a diameter of ~50 μm and shows a distinct donut shape with heights of 0.75 μm at the rim and of 0.1 μm in the center. The observed, unwanted coffee ring effect in inkjet printing technology[24,25] disappears during sintering. Figure 3b shows the same droplet after thermal treatment at 250 °C for 1 min. Single inkjet droplets are arranged as a multiplicity of silver particles instead of a homogeneous layer. A SEM image taken from a thermally sintered droplet also shows the inhomogenous arrangement of the resulting silver feature (Figure 3c).

Printing with a drop spacing of 20 μm gave closed layers with a height of ~1.5 μm. The formation of a crystalline structure in the raw printed layer is shown in Figure 4a. Sintering leads a 150 nm thick silver layer with ripples of ~1 μm height (Figure 4b and Figure 4c). A reason for this could be the volume loss of 90%, which results from the decomposition and evaporation of the organic compounds. This is a known phenomenon in processing MOD inks.[26]

The conductivity of these layers was determined by the four-point method and amounts to 2.7×10^7 S m^{-1}, which corresponds to 43% of the bulk silver conductivity (6.2×10^7 S m^{-1}).[27] Resistance measurements during sintering showed that a 5×0.7 mm^2 printed area (250 °C) is obtained after 30 s. The resistance drops over several magnitudes to 3.4 Ω after 14 s (= initial time) and reaches its final value of 3.0 Ω after 26 s. This shows that thermal decomposition and evaporation of the in situ produced silver nanoparticle protecting organics are accomplished in a significant shorter time continuum than discussed earlier in the TG-MS studies.

Table 1. Mass Spectrometry of Gaseous Products Formed by the Thermal Decomposition of 3

mass number	formula	intensity	comment
12	C^+	3×10^{-12}	MS fragments
13	CH^+	8×10^{-12}	CH_4
14	CH_2^+; N^+	3×10^{-11}	
15	CH_3^+	6×10^{-11}	
16	CH_4^+	6×10^{-11}	
28	CO^+; $C_2H_4^+$	1×10^{-10}	CO
29	CHO^+; $C_2H_5^+$	7×10^{-11}	CH_2O; CH_3OH; C_2H_6
30	CH_2O^+; $C_2H_6^+$	2×10^{-11}	CH_2O; CH_3OH; C_2H_6 CH_3OH; C_2H_6
31	CH_3O^+	2×10^{-11}	O_2
32	O_2^+	2×10^{-11}	
36	Ar^+		atmosphere
38	Ar^+		
39	Ar^+		
42	$C_2H_2O^+$	4×10^{-12}	C_2H_5OH
43	$C_2H_3O^+$	9×10^{-12}	C_2H_5OH
44	CO_2^+	8×10^{-11}	CO_2
45	$C_2H_5O^+$	2×10^{-11}	C_2H_5OH
46	$C_2H_6O^+$	2×10^{-12}	C_2H_5OH
57	$C_2O_2H^+$; $C_3H_5O^+$	2×10^{-12}	CH_3COOH; C_3H_8O
58	$C_2O_2H_2^+$; $C_3H_6O^+$	5×10^{-12}	CH_3COOH; C_3H_8O
59	$C_2O_2H_3^+$; $C_3H_7O^+$	$3 \cdot 10^{-12}$	CH_3COOH; C_3H_8O

(23) (a) Fernandez, E. J.; Garcia-Barrasa, J.; Laguna, A.; Lopez-de-Luzuriaga, J. M.; Monge, M.; Torres, C. *Nanotechnology* **2008**, *19*(18), 185602/1–185602/6. (b) Shim, I.-K.; Lee, Y. I.; Lee, K. J.; Joung, J. *Mater. Chem. Phys.* **2008**, *110*(2−3), 316–321.

(24) Soltman, D.; Subramanian, V. *Langmuir* **2008**, *24*(5), 2224–2231.
(25) Perelaer, J.; Smith, P. J.; Hendriks, C. E.; van den Berg, A. M. J.; Schubert, U. S. *Soft Matter* **2008**, *4*, 1072–1078.
(26) Vest, W. R. In *Ceramic Films and Coatings*; Wachtman, J. D., Haber, R. A., Eds.; Noyes Publications: Park Ridge, NJ, 1993; pp 303−347.
(27) Lide, D. R., Ed. *Handbook of Chemistry and Physics*, 77th ed.; CRC Press, Boca Raton, FL, 1996; pp 12−41.

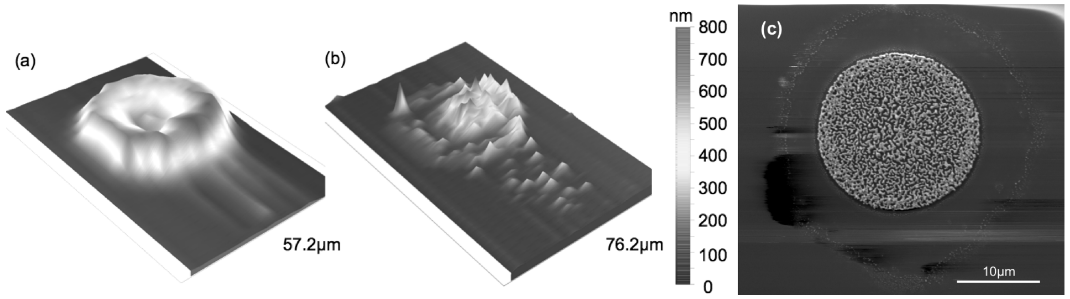

Figure 3. The 3D profilometer image of an inkjet printed (a) dried and (b) sintered (250 °C, 1 min) droplet of an aqueous 23% solution of **3** and (c) SEM image of a sintered (250 °C, 1 min) droplet (size variation due to drop volume deviations while printing).

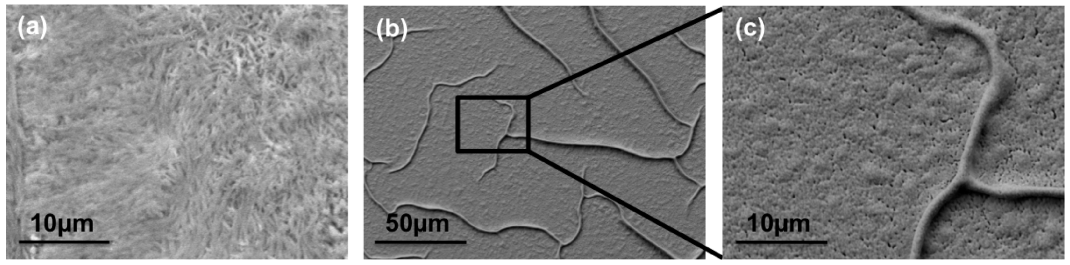

Figure 4. SEM images of (a) a printed layer and (b, c) a sintered silver layer (5 min, 250 °C).

However, for most of the polymeric substrate materials including PET, the needed sintering temperature of 250 °C is too high because they melt or decompose before elemental silver is processed. Therefore, lower sintering temperatures are necessary. When the sinter process is carried out below 250 °C, the transformation process is significantly longer. The initial time for sintering at 130 °C amounts to 60 min, while at 100 °C a time of 252 min is necessary to reach percolation through the appropriate feature; the resistance diminishes below 100 Ω. After 5 h of thermal treatment, conductivities of 0.9×10^7 S m^{-1} (sintering at 130 °C) and 0.4×10^7 S m^{-1} (100 °C) are obtained. In contrast to TG and DSC studies (vide supra) carried out under argon or nitrogen inert gas atmosphere, it was found that the decomposition of **3** to produce conductive silver layers occurs in air at temperatures below 200 °C.

The MOD ink shows a strong absorbance at 350 nm, as indicated by UV−visible measurements. Out of this it seems applicable to combine thermal treatment and UV radiation to improve the sintering process concerning necessary time and final conductivity. Printed structures were irradiated with UV light (70 mW cm^{-2}) during the sintering process. Figure 5 shows the initial time (left) and the final conductivity (right) in dependency of the sintering temperature. From this figure it can be seen that the initial time increases from 43 (at 130 °C) to 68 min (at 100 °C) by lowering the sintering temperature. Sintering at 100 °C led to a conductivity of 0.4×10^7 S m^{-1}, while UV-enhanced sintering gave a value of 1.6×10^7 S m^{-1}.

To prove the adaptability of the MOD ink and the sintering process on polymeric substrates, the concept was applied using PET foil as substrate. The aqueous silver MOD ink was printed onto PET and afterward was sintered at 130 °C with enhancement of UV

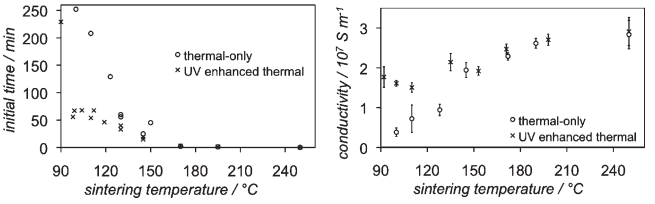

Figure 5. Initial times (left) and final conductivity (right) after 5 h of sintering for thermal and UV-enhanced thermal sintering of **3** depending on the sintering temperature.

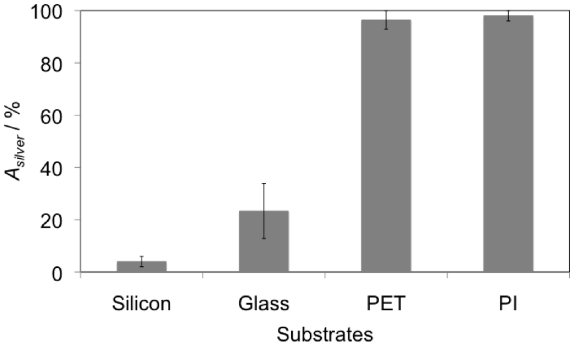

Figure 6. Area coverage A_{silver} of the residual silver layer after three tape laminations.

irradiation. The initial time is ~30 min. The final conductivity amounts to 1.1×10^7 S m^{-1}, which is in accordance with 18% of bulk silver conductivity.

Figure 6 shows the results of the conducted tape tests. Samples on silicon, glass, and polyimide (PI) were sintered thermally, while deposits on PET were converted via UV-enhanced thermal sintering. Substrate surface treatment before printing and thermal annealing was restricted to rinsing with ethanol or isopropanol and deionized water. It was found that on the inorganic substrates (silicon, glass) the sintered silver features show

poor adhesion (4% on silicon, 23% on glass). After the first peel-off from silicon, ~90% of the silver was attached to the tape. On the contemplated polymeric substrates almost no material was removed by the tape and the structures were still conductive after the third lift-off, which is advantageous for practical applications.

3. Conclusions

The reaction of the silver(I) salt [$AgNO_3$] with HO_2C-$(CH_2OCH_2)_3H$ in the presence of triethylamine gave a colorless metal−organic silver(I) 2-[2-(2-methoxyethoxy)-ethoxy]acetate, [$AgO_2C(CH_2OCH_2)_3H$]. From this transition metal complex a 23% aqueous solution was used as MOD ink for piezo inkjet printing. The particle-free ink featuring no additional stabilizing ligands has a silver content of 9.1 wt %. TG-MS studies showed that a sintering temperature of 250 °C is required to obtain conductive silver structures. Inkjet printing was carried out with the Dimatix materials printer DMP 2831. The sintered silver features possess a conductivity of 2.7×10^7 S m^{-1}, which corresponds to 43% of bulk silver conductivity. Sintering at lower temperatures led to conductive layers as well but required more time. It could be shown that sintering below 130 °C is possible but must be assisted by enhancement of UV radiation, as it could be successfully be proven using PET as substrate material. The conductivity of the appropriate silver structures corresponds to 18% of bulk silver. Tape tests proved very good adhesion of the printed and sintered silver patterns on the polymeric substrates.

4. Experimental Section

The silver(I) carboxylate [$AgO_2C(CH_2OCH_2)_3H$] (**3**) was synthesized according to the procedure described by Steffan et al.[22] The MOD ink containing **3** was prepared by dissolving 3.0 g (10.52 mmol) of **3** in 10 mL of water.

TG and DTA measurements were carried out with a simultaneous thermal analyzer (STA 409 Luxx) of NETZSCH Co. The gas outlet of the thermogravimetric analysis device was directly coupled with a mass spectrometer (Äolos, NETZSCH; $(m/z)_{max}$ = 300 amu). Measurements were carried out in the temperature range 25−500 °C with a heating rate of 10 K min^{-1} in an atmosphere of argon. The composition of the gas phase has been detected in the first measurement run with an overall scan in the mass range m/z = 1−300, and fragments of the gaseous species with m/z = 12 (C^+) up to 59 ($C_2O_2H_3^+$) have been detected. A second run of the TG-MS measurement has been performed in order to detect the temperature dependent intensities of the main species CH_3^+ (m/z = 15), CH_4^+ (m/z = 16), CO^+ (m/z = 28), CHO^+ (m/z = 29), and CO_2^+ (m/z = 44). DSC experiments were carried out with the PerkinElmer System Pyris DSC 6 with a constant heating rate of 8 K min^{-1} under N_2 (1.0 cm^3 min^{-1}). Viscosity was determined with a rotational rheometer Physica MCR 51 from Anton Paar at a shear rate of 1,000 s^{-1}, and surface tension was measured by the pendant drop method using a DataPhysics Instruments OCA30 optical contact angle measurement system. A Dimatix materials printer DMP 2831 (FUJIFILM Dimatix, 10 pL print-heads) was used as piezo inkjet printing system. A trapezoid single voltage pulse with a maximum amplitude of 20 V was applied as waveform to the print-head. Printing was conducted under ambient conditions without heating the print-head or the substrate. SEM images were taken with a Hitachi TM1000, and the 3D profiles were recorded with a tactile profilometer DekTak 8 M from Veeco Instruments. Thermal treatment of the samples was carried out using a heating plate VMS-C7 from VWR. UV-enhanced thermal sintering was done by combining thermal treatment with the heating plate with additional UV irradiation with a UV lamp UVA HAND from Hönle. Conductivity was determined by four-point conductivity measurements using a setup including a Prober PM5 from SÜSS MicroTec Test Systems and a 2612 SYSTEM SourceMeter from Keithley Instruments. To investigate the time-dependent resistance while sintering, 10×0.7 mm^2 areas were printed in three layers over two presintered 3×3 mm^2 silver electrodes, whereby the distance of them to each other amounted to 5 mm. The resistance of the features was measured during sintering with a Voltcraft VC840 multimeter at a sampling rate of 1 Hz and was transferred to a PC. The UV absorbance spectrum of the ink was taken with a Cary 100 UV−visible spectrophotometer (Varian Inc.) in a quartz cuvette at an optical path length of 2 mm. The tape test[28] was carried out by printing three layers of 3×3 mm^2 squares onto glass object slides (SuperFrost, Gerhard Menzel, Glasbearbeitungswerk), undoped and polished silicon wafers (⟨100⟩, native oxide), polyimide (PI, Kapton, Dr. D. Müller GmbH) and PET (Melinex, DuPont Teijin Films U.S. Limited Partnership, 125 μm thickness). The sintered squares were laminated with commercial tape (tesafilm, tesa) and peeled off manually after a few seconds. The area coverage of the residual silver layer after three peel-offs was measured optically.

Acknowledgment. We are grateful to the Deutsche Forschungsgemeinschaft (DFG) and the Fonds der Chemischen Industrie for funding this project. We also thank Catharina Meier, Philipp Kitschke, Lars Bernhard, and Maik Müller for many discussions and laboratory assistance.

Supporting Information Available: Graphical illustration of the 1D solid state structure and the space filling model of **3** and their orientation with respect to the unit cell (PDF). This material is available free of charge via the Internet at http://pubs.acs.org.

(28) (a) Shahid, M.; Mazhar, M.; Hamid, M.; O'Brien, P.; Malik, M. A.; Helliwell, M.; Raftery, J. *Dalton Trans.* **2009**, 5487–5494. (b) Xilian, S.; Jianda, S. *Appl. Surf. Sci.* **2006**, *253*, 2093–2095. (c) Gadre, K. S.; Alford, T. L. *J. Appl. Phys.* **2003**, *93*(2), 919–923.